

Constraint Operator for the Kinematic Calibration of a Parallel Mechanism

Min Ki Lee*, Tae Sung Kim

*Department of Control and Instrumentation Engineers Changwon National University,
Kyungnam 641-773, Korea*

Kun Woo Park, Sung Ha Kwon

School of Mechatronics Engineering Changwon National University, Kyungnam 641-773, Korea

This paper introduces a constraint operator for the kinematic calibration of a parallel mechanism. By adopting the concept of a constraint operator, the movement between two poses is constrained. When the constrained movements are satisfied, the active joint displacements are taken and inputted into the kinematic model to compute the theoretical movements. A cost function is derived by the errors between the theoretical movement and the actual movement. The parameters that minimize the cost function are estimated and substituted into the kinematic model for a kinematic calibration. A single constraint plane is employed as a mechanical fixture to constrain the movement, and three digital indicators are used as the sensing devices to determine whether the constrained movement is satisfied. This calibration system represents an effective, low cost and feasible technique for a parallel mechanism. A calibration algorithm is developed with a constraint operator and implemented on a parallel manipulator constructed for a machining center tool.

Key Words: Constraint Operator, Calibration, Cost Function, Constraint Plane, Digital Indicator, Kinematic Parameter, Observability, Position/Velocity Control

1. Introduction

Kinematic calibration is the identification of actual parameters of a kinematic model residing in the manipulator controller. It is achieved through the following steps: 1) analyzing forward and inverse kinematics; 2) deriving the cost function from the errors between the theoretical movement and actual movement; 3) estimating actual kinematic parameters to minimize the cost function. Among the above steps, kinematic analysis and estimation technique are no longer obstacles since computation techniques have become quite powerful, but the technique that

measures the actual movement is still an issue.

For the calibration of a parallel mechanism, the actual pose of the platform is acquired by external measuring devices such as laser (Zhuang et al., 1992a), theodolite (Masory and Jiahua, 1995) and inclinometer (Desnard and Khalil, 1999). These methods can directly measure the platform pose that is the calibration target, but it is expensive and difficult to obtain accurate calibration data in the 3D space. Zhuang (Zhuang, 1997) and Wampler, et al. (Wampler et al., 1995) have proposed the methods that indirectly measure the platform pose from passive joint displacements rotated or translated in accordance with the platform pose. These methods make a self and on-line calibration possible by internal sensing, but it is neither practical nor economical to install redundant sensors at passive joints. Also it is doubtful that some of the measured passive joints can correctly represent the platform pose.

* Corresponding Author,

E-mail: minkilee@sarim.changwon.ac.kr

TEL: +82-55-279-7553; **FAX:** +82-55-262-5064

School of Mechatronics Engr. Changwon National University, Kyungnam 641-773, Korea. (Manuscript Received November 28, 2001; Revised October 22, 2002)

The purpose of the pose measurement is to find the error in the theoretical pose computed from a kinematic model. Here, a new approach for identifying the error is considered: 1) constrained movements are established; 2) active joint displacements are read when a platform satisfies the constrained movements; 3) the active joint displacements are substituted into a kinematic model to compute the theoretical movement; 4) the error is computed by subtracting the theoretical movement from the pre-established constrained movement. A variety of constraints can be selected: A robot pose is constrained by docking the robot end-effector into a pin fixture (Veitscherrer and Wu, 1988) and some of the coordinates are restricted by points (Bennett and Hollerbach, 1991) or planes (Zhuang et al., 1999). These are equivalent to measurements of the coordinates of the end-effector by the external measuring sensors. Calibration with the constraints needs only a simple sensing device to check whether the constrained movements are satisfied within an established range. But the constrained movements must be chosen to assure the observability for all kinematic parameters embedded in a cost function (Zhuang et al., 1992b).

The calibration methods reviewed above have been applied to simulated motion of parallel and serial robot manipulators. A few methods (Masory and Jiahua, 1995; Wampler et al., 1995) are implemented in actual systems but their calibration results failed to reach the accuracy that a machining center tool requires. This research derives a calibration algorithm through the definition of a constraint operator and applies it to a PMCT (Lee et al., 2000) (Parallel typed Machining Center Tool) constructed for a machining tool. The characteristics of the parallel mechanism are elucidated by comparing the simulation results with experimental results.

2. Definition of a Constraint Operator

Forward kinematics of the parallel manipulator is expressed by

$$\boldsymbol{x} = f(\boldsymbol{\rho}, \boldsymbol{q}) \quad (1)$$

where $\boldsymbol{x} = [\boldsymbol{\Omega}^T, \boldsymbol{p}^T]^T$ is a 6×1 vector defining the platform pose: $\boldsymbol{\Omega} = [\Omega_x, \Omega_y, \Omega_z]^T$ and $\boldsymbol{p} = [p_x, p_y, p_z]^T$ are a set of Euler angles and a position vector of platform, respectively. The equation provides the platform pose for a given set of kinematic parameter vector, $\boldsymbol{\rho}$ and active joint displacement vector, \boldsymbol{q} . The platform can be located arbitrarily at unconstrained coordinates but it must be restricted in constrained coordinates. Here, *twist* coordinates are employed to describe a constrained movement (Hunt, 1978). While a body is moving in space, its movement is represented by 6-components of *twist* coordinates:

$$\boldsymbol{T} = [T_1, T_2, T_3, T_4, T_5, T_6]^T \quad (2)$$

where T_1, T_2 and T_3 are the components of the angular velocity of the body, and T_4, T_5 and T_6 are those of the linear velocity. The constraint is to specify the constrained coordinates and the quantity of movement. A constraint operator, \boldsymbol{C} $[\cdot]$ is defined to constrain the movement between two poses in bracket, $[\cdot]$. When a platform moves from \boldsymbol{x}_u to \boldsymbol{x}_v under \boldsymbol{C} , the constrained movement is written as

$$\boldsymbol{C}[\boldsymbol{x}_v - \boldsymbol{x}_u] = \boldsymbol{N} \quad (3)$$

where

$$\boldsymbol{C} = \text{diag}(c_1, c_2, \dots, c_6)$$

$$\boldsymbol{N} = [n_1, n_2, \dots, n_6]^T$$

$c_j (j=1, 2, \dots, 6)$ is "1" if j -th coordinate of *twist* is constrained, and if not constrained, it is "0", and $n_j (j=1, 2, \dots, 6)$ is defined by

$$n_j = 0 \text{ for } c_j = 0 \quad (4a)$$

$$n_j = {}^d n_j + \hat{n}_j \text{ for } c_j = 1 \quad (4b)$$

where ${}^d n_j$ is the established quantity of the movement and \hat{n}_j is the deviation from the established quantity, which may be a constraint fixture error, a measurement noise, etc.. The number of constrained coordinates is determined by $k = \sum_{j=1}^6 c_j$.

That is, $\boldsymbol{C} = [0, 0, \dots, 0]^T$ for all coordinates unconstrained implies that the platform moves free, and $\boldsymbol{C} = [1, 1, \dots, 1]^T$ for all those constrained implies that the platform docks into a pin fixture.

3. Error Model

An error model with a constraint operator is derived from Eq. (3). When a constrained movement occurs from \mathbf{x}_0 to \mathbf{x}_i , it will be expressed by

$$\Psi_a(\boldsymbol{\rho}, \Delta^m \mathbf{q}_i) \equiv C[f(\boldsymbol{\rho}, {}^m \mathbf{q}_i) - f(\boldsymbol{\rho}, {}^m \mathbf{q}_0)] = N_i \quad (5)$$

where

$$\Delta^m \mathbf{q}_i = {}^m \mathbf{q}_i - {}^m \mathbf{q}_0$$

and ${}^m \mathbf{q}_0$ and ${}^m \mathbf{q}_i$ are the active joint displacement vectors at the initial pose and i -th pose, respectively, when the platform satisfies the constraint movements. A subset of N_i is defined by a $k \times 1$ vector $\boldsymbol{\Gamma}_i$ that is composed of the constrained coordinates. A vector, $\boldsymbol{\Gamma}_i$ is expressed by a function Ψ as follows:

$$\boldsymbol{\Gamma}_i = \Psi(\boldsymbol{\rho}, \Delta^m \mathbf{q}_i) \quad (6)$$

This equation denotes the constrained quantity of movement between two poses under C . The quantity can be computed by applying $\Delta^m \mathbf{q}_i$ into a kinematic model:

$${}^c \boldsymbol{\Gamma}_i = \Psi(\boldsymbol{\rho}^0, \Delta^m \mathbf{q}_i) \quad (7)$$

where $\boldsymbol{\rho}^0$ is a parameter vector in the kinematic model. The solutions from Eqs. (6) and (7) must be equal because the manipulator is identical. However, $\boldsymbol{\Gamma}_i$ is different from ${}^c \boldsymbol{\Gamma}_i$ because $\boldsymbol{\rho}^0 \neq \boldsymbol{\rho}$, which yields the error vector $\Delta \boldsymbol{\Gamma}_i = \boldsymbol{\Gamma}_i - {}^c \boldsymbol{\Gamma}_i$. If $d\boldsymbol{\rho} = \boldsymbol{\rho} - \boldsymbol{\rho}^0$ is substituted Eq. (6) is rewritten as

$$\boldsymbol{\Gamma}_i = \Psi(\boldsymbol{\rho}^0 + d\boldsymbol{\rho}, \Delta^m \mathbf{q}_i) \quad (8)$$

If $d\boldsymbol{\rho}$ is sufficiently small, we can drop the second and higher order terms in a Taylor expansion as follows:

$$\boldsymbol{\Gamma}_i \cong \Psi(\boldsymbol{\rho}^0, \Delta^m \mathbf{q}_i) + {}^i \mathbf{J}_\Psi d\boldsymbol{\rho} \quad (9)$$

where ${}^i \mathbf{J}_\Psi \equiv \nabla \Psi$ and ${}^i \mathbf{J}_\Psi$ is a Jacobian of Ψ with respect to $\boldsymbol{\rho}$. Subtracting Eq. (7) from (9) gives

$$\Delta \boldsymbol{\Gamma}_i \cong {}^i \mathbf{J}_\Psi d\boldsymbol{\rho} \quad (10)$$

The main objective behind deriving the error model is to estimate parameter errors. To achieve

this objective, a cost function can be defined in terms of the error model given above:

$$C_\Psi(\boldsymbol{\rho}) = \sum_{i=1}^p [\Delta \boldsymbol{\Gamma}_i - {}^i \mathbf{J}_\Psi d\boldsymbol{\rho}]^T [\Delta \boldsymbol{\Gamma}_i - {}^i \mathbf{J}_\Psi d\boldsymbol{\rho}] \quad (11)$$

where $C_\Psi(\boldsymbol{\rho})$ is a cost function of $\boldsymbol{\rho}$ and p is the number of calibration data. Referring to Eq. (10), the maximum number of independent error equations is $(p \times k)$. As a rule of thumb (Wampler et al., 1995), twice as many as the required number of kinematic parameters need to be used for kinematic identification. If the number of error equations is insufficient, the identification Jacobian is rank-deficient and the cost function will not involve all kinematic parameters. If a sufficient number of the error equations is obtained to enhance the parameter observability, nonlinear optimal techniques such as the Gauss-Newton, the Levenberg-Marquardt algorithms and the Extended Kalman filter are applied to find the actual parameter vector $\boldsymbol{\rho}$ that minimizes the cost function down to a desired limit.

4. Application of Calibration Algorithm to the PMCT

The calibration algorithm derived in the previous section is applied to the PMCT (Lee et al., 2000). A variety of parallel manipulators are developed to solve the small workspace of the parallel mechanism (Lee and Park, 1999). But it is known that any device designed by modifying the Stewart Platform reduces stiffness so that the PMCT is constructed on the basis of the Stewart Platform as shown in Fig. 1(a).

The PMCT is made up of a fixed base, a mobile platform and six linear actuators, LA_ i for $i=1, 2, \dots, 6$. As shown in Fig. 1(b), the LA_ i is attached to B_i through a ball-socket joint and connected to P_i through a universal joint constituting link trains which possess six degrees of freedom. To increase the stiffness, the distance of $\| \overline{B_i P_i} \|$ is shortened by holding the mid-allocation of LA_ i with the ball-socket joint. Five rotary joints (ball-socket joint and universal joint) are all passive joints and only one prismatic joint is an active joint to extend or shorten

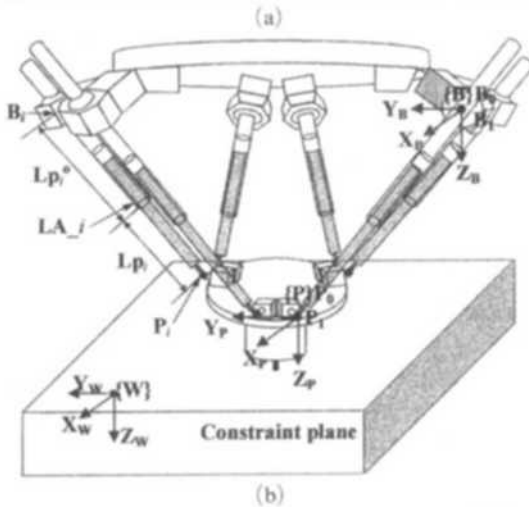
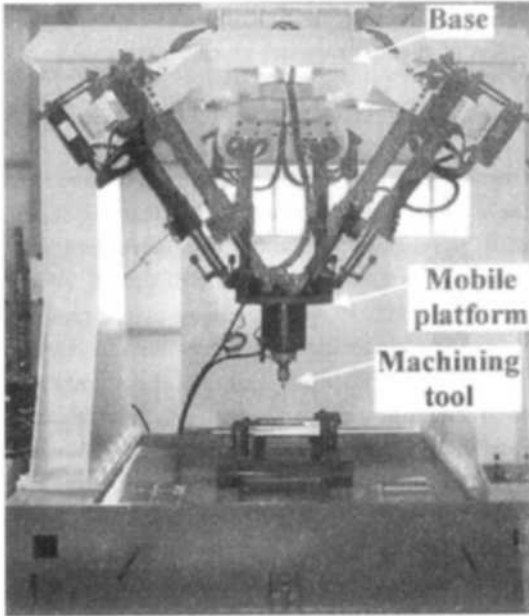


Fig. 1 (a) The PMCT constructed for a machining center tool (b) Kinematic structure

the length of LA_i . This linear actuation places the platform at a desired pose.

For the calibration, let us define the Cartesian coordinate frames and kinematic parameters. The calibration data are measured with respect to the constraint plane and transformed to those of the PMCT. For a world reference, the frame $\{W\}$ is assigned to the constraint plane: Z_w is perpendicular to the constraint plane, and both X_w and Y_w are parallel with the plane and its origin

is arbitrarily located on the plane. In addition, frames $\{B\}$ and $\{P\}$ are fixed to the base and the platform, respectively, and their origins are located on points B_1 and P_1 , respectively. The orientation of $\{B\}$ is defined to be identical with that of $\{W\}$ and in a home position, the orientations of $\{P\}$ and $\{B\}$ are also identical. The external sensors (Zhuang et al., 1992a; Masory and Jia-hua, 1995; Desnard and Khalil, 1999) such as digital indicators need six parameters to transform the calibration data measured with respect to an environmental frame to those of the manipulators. However, the frames defined above do not require any other parameter except for the PMCT kinematic parameters since the orientations of $\{W\}$ and $\{B\}$ are identical and the relative constrained movements between poses are used as the calibration data. Hence the calibration is conducted with respect to the constraint plane located arbitrarily in a workspace.

The platform's position and orientation are expressed by a 3×1 vector, ${}^B\vec{B}_0\vec{P}_0$ and a 3×3 rotation matrix of $\{P\}$ with respect to $\{B\}$, ${}^B R_P$ respectively. Hence, the total number of parameters involved in the kinematic model is 42, i.e., ${}^B\vec{B}_0\vec{B}_i$, ${}^P\vec{P}_0\vec{P}_i$, Lp_i^0 for $i=1, 2, \dots, 6$. Here Lp_i^0 is an initial length of LA_i and active joint displacements, Lp_i is computed by $Lp_i = \|\vec{B}_i\vec{P}_i\| - Lp_i^0$. The definition of $\{B\}$ and $\{P\}$ gives

$${}^B B_{1x} = {}^B B_{1y} = {}^B B_{1z} = 0 \quad (12a)$$

$${}^P P_{1x} = {}^P P_{1y} = {}^P P_{1z} = 0 \quad (12b)$$

where ${}^i V_{jk}$ is the coordinate of k axis of point V_j with respect to frame $\{i\}$. These equations reduce the number of parameters down to 36 given as a set of kinematic parameters defined by

$$\rho = [{}^B B_{2x}, {}^B B_{2y}, {}^B B_{2z}, \dots, {}^P P_{6x}, {}^P P_{6y}, {}^P P_{6z}, Lp_1^0, Lp_2^0, \dots, Lp_6^0]^T \quad (13a)$$

A set of active joint displacements is defined by

$$q = [Lp_1, Lp_2, Lp_3, Lp_4, Lp_5, Lp_6]^T \quad (13b)$$

In order to constrain the platform movement, we place a constraint plane of dimension $400 \times 400 \text{ mm}^2$ with a flatness of $5 \mu\text{m}$ below the mobile platform, which isn't necessarily parallel to a

fixed base. The sensing device used to inspect the constrained movement is a digital indicator whose resolution and stroke are $1 \mu\text{m}$ and 25 mm , respectively. The kinematic parameters are calibrated with respect to a single constraint plane so that they are accommodated to the misalignment of the plane.

For the constrained movements, let us take three constrained coordinates such as one position coordinate and two orientational coordinates of the platform. Three digital indicators are mounted symmetrically 120° apart on a platform to inspect the movement in Z_B axis. Since the constraint plane is flat, the indicator readings change when the platform rotates about X_B and Y_B axes, and translates along Z_B axes. Therefore, if the platform moves from an initial pose to i -th pose without changing the reading of any of the three indicators, these three coordinates are constrained. This constraint can be expressed by a constraint operator, $C = \text{diag}(1, 1, 0, 0, 0, 1)$ which means that the first, the second and the sixth coordinates out of the twist coordinates, i.e., Ω_x , Ω_y and p_z , are constrained.

The magnitude of the movement between two poses is established by ${}^d n_1 = {}^d n_2 = {}^d n_6 = 0$ because the constraint plane is flat. The deviations from the established magnitude are $\hat{n}_1 = \hat{n}_2 = \hat{n}_6 = 0$ under the assumption that there is neither fixture error nor measurement noise. If a platform moves from \boldsymbol{x}_0 to \boldsymbol{x}_i while maintaining the indicator readings unchanged, the constrained movement is given by

$$\boldsymbol{\Gamma}_i = [\Delta^c \Omega_x, \Delta^c \Omega_y, \Delta^c p_z]^T = [0, 0, 0]^T \quad (14)$$

A theoretical movement with $\Delta^m \boldsymbol{q}_i$ and $\boldsymbol{\rho}^0$ is computed by

$${}^c \boldsymbol{\Gamma}_i = [\Delta^c \Omega_x, \Delta^c \Omega_y, \Delta^c p_z]^T = \boldsymbol{\Psi}(\boldsymbol{\rho}^0, \Delta^m \boldsymbol{q}_i) \quad (15)$$

Three equations are obtained from one constrained movement. Twice as many as the required number of kinematic parameters need to be used for kinematic identification. Thus, 25-constrained movements are generated to estimate the kinematic parameters.

Before the calibration, the repeatability and accuracy of the PMCT are inspected. We substi-

Table 1 Design of kinematic parameters (unit : mm)

i	${}^B B_0 B_i$			${}^P P_0 P_i$			$L p_i^0$
	X	Y	Z	X	Y	Z	
1	0	0	0	0	0	0	850
2	-345.18	-199.29	0	-318.43	-183.84	0	850
3	-1288.23	345.18	0	-434.98	-116.55	0	850
4	-1288.23	743.76	0	-434.98	251.14	0	850
5	-345.18	1288.23	0	-318.43	318.43	0	850
6	0	1088.94	0	0	134.58	0	850

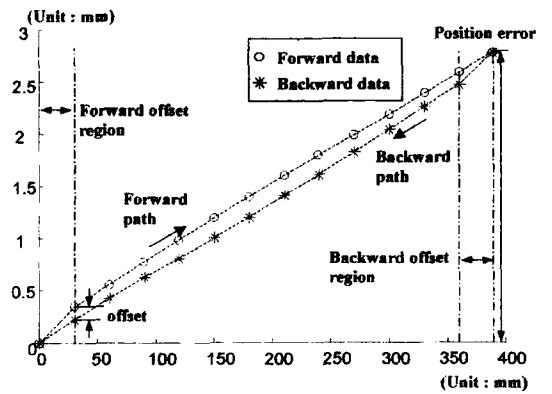


Fig. 2 Hysteresis curve formed by the position error difference between forward and backward paths

tute the design parameters shown in Table 1 into a kinematic model and move the platform thirteen times in 30 mm increments along (+) X axis and return to the initial location with the same commands along (-) X axis. These movements are repeated three times and the distance of a target mounted on the platform is measured by a laser sensor.

As shown in Fig. 2, the error starts increasing and its rate kept constant beyond the starting region. In return movement, the error decreases back to zero. If a platform approaches the inspected locations along the same direction, the repeatability is kept within $2 \mu\text{m}$ but it increases to $200 \mu\text{m}$ along the different direction, thus yielding a hysteresis curve. The offset of $200 \mu\text{m}$ is due to joint backlashes, which induce the constrained movements not to be generated in accordance with a geometric model. The backlashes

predominantly cause the errors in the backlash region but beyond that, the wrong parameters assigned in the kinematic model yield errors with a uniform rate.

A simulation is performed to examine the observability of the method proposed above. The initial parameters are chosen as the design parameters. The errors of Lp_i^0 are kept within ± 5 mm and those of ${}^B B_0 B_i$ and ${}^P P_0 P_i$ to within ± 3 mm. Levenberg-Marquardt algorithm is used to estimate the kinematic parameters. As shown in Fig. 3, $C_{\mathcal{V}}(\rho)$ converges to zero.

The calibration algorithm is applied to the PMCT as it has been applied to the simulation. The calibration data are obtained from 25-sectors distributed evenly over the constraint plane. A platform moves from \mathbf{x}_0 to $\mathbf{x}_i (i=1, 2, \dots, 25)$ while performing the readings of three digital indicators. When the changes of all the readings fall within $\pm 2 \mu\text{m}$, the changes of active joint displacements, $\Delta^m \mathbf{q}_i$ are provided as the calibration data. The platform moves to each successive pose under velocity control. To ensure that each reading of the indicators falls within a desired range, the velocity in the desired direction is produced by pushing the corresponding key. The velocity control is easily accomplished by operating a keyboard or a joystick intuitively without a feedback measurement and a concomitant computation burden. We estimate the kinematic parameters that minimizing a given cost function with calibration data.

Since the actual kinematic parameters are unknown, we can evaluate the calibration performance by the convergence of $C_{\mathcal{V}}(\rho)$. As shown in Fig. 3, $C_{\mathcal{V}}(\rho)$ at the PMCT isn't reduced below 0.05. This poor convergence comes from the velocity control to generate the constrained movements. During the precise movement control, the movement directions are changed several times so that large backlashes and measurement noise are involved in the calibration data.

The poses are regenerated with the calibration data to inspect how well the constraint conditions are satisfied. The indicator readings are over $\pm 200 \mu\text{m}$. This implies that the calibration data are significantly contaminated. Consequent-

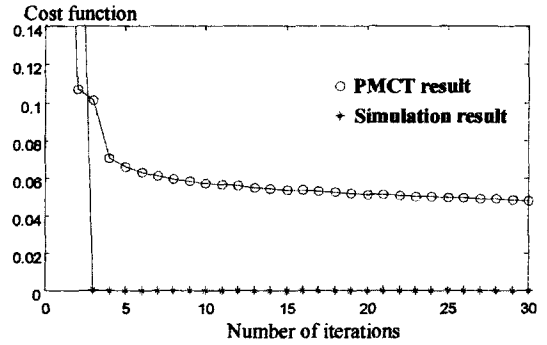


Fig. 3 Cost function vs. number of iterations

ly, $C_{\mathcal{V}}(\rho)$ of the PMCT could not converge well in comparison with that of the simulation.

To minimize the backlash effect, a platform repeatedly moves up and down in the center of the workspace, which gets rid of backlashes from the other directions except for the upward/downward direction. We keep the approach direction consistent to the calibration data by always starting from the center of the workspace. The directional change from the center to the constrained pose may cause backlashes, which arise from beyond the backlash region but they remain constant as shown in Fig. 2. The error model is derived from the relative movement between two constrained poses so that the same quantity of backlashes involved in the calibration data cancel out.

A position control is implemented to generate the constrained movement in the minimum number of directional changes. The position control requires a feedback measurement of the calibration data and additional computation to compute the active joint displacements needed to reduce the deviations in the minimum number of steps: three indicator deviations, $\{\Delta D_1, \Delta D_2, \Delta D_3\}$ from the established range are measured and feedback to the controller which computes the control lengths of LA_i , $\{\Delta Lp_1, \Delta Lp_2, \dots, \Delta Lp_6\}$ needed to make the deviations to be $\{0, 0, 0\}$. For this, a 3×6 Jacobian matrix, J_d is empirically obtained by relating the changes in the digital values with respect to the changes in the lengths of LA_i . Then, the lengths of LA_i needed to generate the constrained movement is computed by

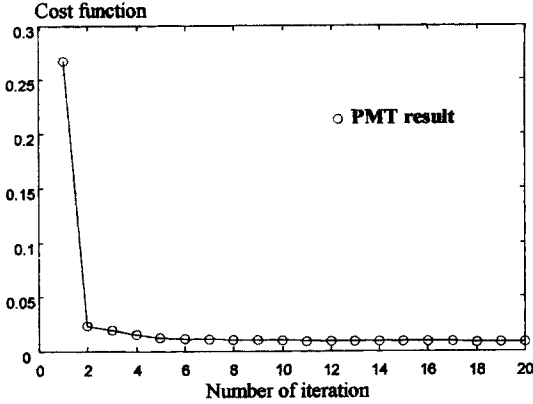


Fig. 4 Cost function vs. number of iterations with calibration data obtained by position control

$$\begin{aligned} & \{ \Delta L p_1, \Delta L p_2, \dots, \Delta L p_6 \}^T \\ & = (\mathbf{J}_d^T \mathbf{J}_d)^{-1} \mathbf{J}_d^T \{ \Delta D_1, \Delta D_2, \Delta D_3 \}^T \end{aligned} \quad (16)$$

All the linear actuations are conducted by a position control and their directional changes keep at minimum to eliminate the backlash effect. Owing to a pseudo inverse in Eq. (16), we cannot reduce the deviation of indicator readings to fall below $30 \mu\text{m}$. For a square Jacobian, $(\Delta L p_1, \Delta L p_3, \Delta L p_5)$ are taken and the deviation range of the readings is established to be $10 \mu\text{m}$. This range is obtained in two directional changes. When the poses are regenerated with the calibration data, the deviation of the indicator readings fall to within $\pm 20 \mu\text{m}$, which represents an improvement by a factor of ten compared with the data obtained by a velocity control. Figure 4 depicts the calibration results through the position control. A cost function, $C_{\mathcal{F}}(\rho)$ converges to 0.01 within 4 iterations. Although a larger tolerance is established for the deviation of indicator readings, the convergence is improved by a factor of four compared with the previous results owing to the minimized backlash effect. Table 2 indicates the estimated kinematic parameters: There is 2–3 mm difference between the calibrated parameters and the designed parameters values. This implies that the PMCT is incapable of meeting the accuracy to within $10 \mu\text{m}$ without the calibration.

To investigate the performance of the calibration system, we give the commands to move the

Table 2 Kinematic parameters obtained by calibration process (unit: mm)

i	${}^B B_0 \vec{B}_i$			${}^P P_0 \vec{P}_i$			$L p_i^0$
	X	Y	Z	X	Y	Z	
1	0	0	0	0	0	0	850.12
2	-345.40	-198.78	-1.44	-319.60	-184.73	1.3	848.04
3	-1287.37	344.00	1.04	-437.02	-116.26	-0.18	851.93
4	-1286.92	743.71	1.19	-436.49	251.72	-1.09	848.44
5	-344.45	1287.84	-1.1	-321.19	318.64	0.48	851.75
6	-0.62	1089.02	-2.74	0.49	133.94	2.53	850.55

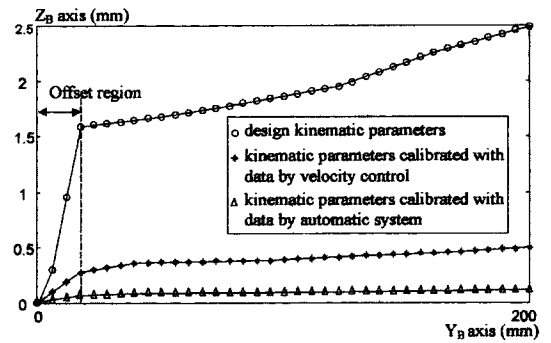


Fig. 5 Calibration results

platform by 200 mm along Y_B axis while allowing no movement along Z_B axis as shown in Fig. 5. The error with the design parameters is 2.5 mm but it is reduced to 0.5 mm with the calibrated parameters through the velocity control. The calibrated parameters through the position control decrease the error down to 0.13 mm. Furthermore, the error beyond the backlash region is to within $20 \mu\text{m}$ satisfying the required accuracy of a machining center tool. However, we still have many problems to apply the PMCT to a machining tool. They can be solved by the improved techniques such as the enhanced accuracy for the constraint fixture, cancellation of measurement noises, compensation of backlashes, etc..

5. Conclusion

The calibration algorithm is developed and implemented to the PMCT constructed for a machining center tool. By adopting the concept of a constraint operator, the movement between two

poses is constrained. When the constrained movements are satisfied, the active joint displacements are computed and inputted into a kinematic model to compute the theoretical movements. A cost function is derived based on the errors between the theoretical movement and the actual movement. The parameters that minimize the cost function are estimated and substituted into the kinematic model for the calibration. A planar table is employed as a mechanical fixture to constrain the movable platform and three digital indicators are used for the sensing devices to detect whether the constrained movement is satisfied. This calibration system represents an effective, low cost, and feasible technique for a parallel typed machining tool in an industrial environment. The planar table with three indicators constrains three coordinates, yielding three independent error equations for one calibration measurement, which are the rotations about X_B and Y_B axes and the translation in Z_B axis. These constraints successfully provide for parameter observability.

To reduce the backlash effects, the position control is implemented to generate the constrained movement with a minimum number of directional changes and to keep the approach direction consistent with the calibration pose. The calibration system with the position control improves the accuracy of the PMCT up to the resolution of $130\ \mu\text{m}$ in the translation of $200\ \text{mm}$. This improvement is remarkable but it doesn't meet the required accuracy of a machining tool. There still exists a backlash region in which passive joints cannot be rotated according to a given geometric constraint. Fortunately, the accuracy beyond the backlash region is reduced to $20\ \mu\text{m}$ and the repeatability to $2\ \mu\text{m}$. To improve the calibration results, future studies need to be conducted to estimate and compensate backlashes and to cancel measurement noise in the parallel mechanism.

Acknowledgment

This work was supported (in part) by the Korea Science and Engineering Foundation

(KOSEF) through the Machine Tool Research Center at Changwon National University.

References

- Bennett, D. and Hollerbach, J. M., 1991, "Autonomous Calibration of Single-loop Closed Kinematic Chains Formed by Manipulators with Passive Endpoint Constraints," *IEEE Trans. Robot. Automat.*, Vol. 7, pp. 597~606.
- Desnard, S. and Khalil, W., 1999, "Calibration of Parallel Robots Using two Inclinometers," *Proc. of the 1999 IEEE Int. Conf. on Robot. Automat. Detroit, Michigan*, pp. 1758~1763.
- Hunt, K. H., 1978, *Kinematic Geometry of Mechanisms*, Oxford Univ. Press.
- Lee, M. K. and Park, K. W., 1999, "Kinematic and Dynamic Analysis of A Double Parallel Manipulator for Enlarging Workspace and Avoiding Singularities," *IEEE Trans. Robot. Automat.*, Vol. 15, No. 6, pp. 1024~1034.
- Lee, M. K., Kim, T. S. and Park, K. W., 2000, "Development of a CNC Machining Tool with Stewart Platform," *Proc. of the ISIM 2000*, Kyongnam, Korea, pp. 270~274.
- Masory, O. and Jiahua, Y., 1995, "Measurement of Pose Repeatability of Stewart Platform," *J. Robot. Syst.*, Vol. 12, No. 12, pp. 821~832.
- Veitscherrer, W. K. and Wu, C. H., 1988, "Robot Calibration and Compensation," *IEEE Trans. Robot. Automat.*, Vol. 4, No. 6, pp. 643~655.
- Wampler, W. Hollerbach, J. M. and Arai, T., 1995, "An Implicit Loop Method for Kinematic Calibration and Its Application to Closed-Chain Mechanisms," *IEEE Trans. Robot. Automat.*, Vol. 11, pp. 710~724.
- Zhuang, H. Li, B. Roth, Z. S. and Xire, X., 1992a, "Self-Calibration and Mirror Center Offset Elimination of a Multi-beam Laser Tracing System," *Robot. Autonomous Syst.*, Vol. 9, pp. 255~269.
- Zhuang, H. Roth, Z. S. and Hamano, F., 1992b, "Observability Issues in Kinematic Error Parameter Identification of Manipulators," *J. Dyn. Sys. Meas. Control. Trans. ASME*, Vol. 114, pp. 319~322.
- Zhuang, H., 1997, "Self Calibration of Parallel

Mechanisms with a Case Study on Stewart Platform," *IEEE Trans. Robot. Automat.*, Vol. 13, pp. 387~397.

Zhuang, H. Motaghedi, S. H. and Roth, Z. S.,

1999, "Robot Calibration with Planar Constraints," *Proc. of the 1999 IEEE Int. Conf. on Robot. Automat.* Detroit, Michigan, pp. 805~810.